

Northumbria Research Link

Citation: Gouda, M. M., Underwood, Chris and Danaher, Sean (2002) Modelling the robustness properties of HVAC plant under feedback control. Building Services Engineering Research and Technology, 24 (4). pp. 271-280. ISSN 01436244

Published by: Sage

URL: <http://dx.doi.org/10.1191/0143624403bt077oa>
<<http://dx.doi.org/10.1191/0143624403bt077oa>>

This version was downloaded from Northumbria Research Link:
<https://nrl.northumbria.ac.uk/id/eprint/224/>

Northumbria University has developed Northumbria Research Link (NRL) to enable users to access the University's research output. Copyright © and moral rights for items on NRL are retained by the individual author(s) and/or other copyright owners. Single copies of full items can be reproduced, displayed or performed, and given to third parties in any format or medium for personal research or study, educational, or not-for-profit purposes without prior permission or charge, provided the authors, title and full bibliographic details are given, as well as a hyperlink and/or URL to the original metadata page. The content must not be changed in any way. Full items must not be sold commercially in any format or medium without formal permission of the copyright holder. The full policy is available online: <http://nrl.northumbria.ac.uk/policies.html>

This document may differ from the final, published version of the research and has been made available online in accordance with publisher policies. To read and/or cite from the published version of the research, please visit the publisher's website (a subscription may be required.)

Modelling the robustness properties of HVAC plant under feedback control

MM Gouda^a BSc MSc PhD, **CP Underwood**^b BSc PhD CEng MCIBSE MASHRAE and **S Danaher**^a BSc PhD CPhys CEng MIEE

^aSchool of Engineering, Northumbria University, Newcastle upon Tyne, UK

^bSchool of the Built Environment and Sustainable Cities Research Institute, University of Northumbria, Newcastle upon Tyne, UK

Most existing building simulation programs fail to capture sufficient of the underlying dynamics of nonlinear HVAC plant and some have restricted room space modelling capabilities for low-time-horizon analyses. In this work, a simplified model of a room space with hot water heating and a chilled ceiling system is developed for the main purpose of analysing control system response. The room model is based on a new approach to lumped capacitance modelling and the heating and chilled ceiling emitters are modelled using third-order descriptions. Control system components are treated in detail and both controllers are 'tuned' at a nominal region of plant operation using a gradient-descent-based optimization procedure. Robustness qualities of the controllers are analysed with reference to extremes in plant operating conditions. A key feature of the work is the transparency of the modelling procedure, designed to have appeal to researchers as well as practitioners involved with HVAC control system design problems.

1 Introduction

There have been a number of developments in modular simulation programs with emphasis on HVAC plant and control, the three most prominent being TRNSYS,¹ HVACSIM+² and SIMBAD.³ TRNSYS has appeal due to the ease with which components can be developed by the user and slotted into whole system simulations (e.g., Underwood⁴) while HVACSIM+ has been used extensively for investigating a wide range of HVAC control problems (e.g., Dexter *et al.*,⁵ Metcalf *et al.*⁶). One restriction with these modular programs is that many of the plant component

models are steady-state or quasi-steady-state, making them suitable (and computationally efficient) for low frequency dynamic analysis but unsuitable for high frequency disturbances, which are important in many instances for control design. A further difficulty lies in the response-factor-based treatment of room spaces with these modular programs which further contributes to their unsuitability for low time horizon modelling. SIMBAD, a relative newcomer, has a more appealing room space modelling approach for HVAC plant and control investigations but many of the available components lack generality at present.

In other avenues of modelling progress for HVAC plant and control, Adams and Holmes⁷ first considered component model description appropriate to HVAC control synthesis. Their work has been restricted to linear transfer functions of key components in HVAC systems such as sensors, coils and heat emitters. Nevertheless, this work produced some of the first component-

Address for correspondence: Chris Underwood, School of the Built Environment and Sustainable Cities Research Institute, University of Northumbria, Newcastle upon Tyne NE1 8ST, UK. E-mail: chris.underwood@unn.ac.uk

First presented at System Simulation in Buildings, Sixth International Conference, 16–18 December 2002. University of Liège, Belgium.

based models enabling stability and response analysis of HVAC systems. A variety of workers have since considered the essentially nonlinear HVAC control problem through bespoke simulations (e.g., Shavit and Brandt,⁸ Brath *et al.*,⁹ and Underwood and Crawford,¹⁰ but these results tend to lack generality.

What is needed is a modelling framework for the specific case of HVAC plant and control which has both flexibility, rigour, computational efficiency and transparency. Accordingly, the objectives of this work were to develop a simulation modelling procedure for HVAC plant and control (including a room space) that permits control system simulations at low time horizons, whilst addressing these features. The model has been developed in Matlab-Simulink affording a high degree of flexibility, functionality and transparency. The vehicle for this has been a relatively new approach to heating and cooling buildings in which precise comfort conditions in summer at least are not of prime concern—embedded chilled ceilings for summer cooling with hot water convector radiators for winter heating are used.

2 Building space modelling—a new approach

Lumped capacitance models of building envelopes have established themselves as computationally-efficient approaches that have sufficient accuracy for short-time-horizon investigations. Early developments have been due to Lorenz and Masy¹¹ and Tindale.¹² However, these low-order model developments have been found to break down in certain instances, in particular when modelling heat transfer through high thermal capacity elements. Gouda *et al.* proposed a new procedure for the element modelling of room spaces based on lumped capacitances through the use of constrained optimization.¹³ Though this resulted in second-order descriptions for each room envelope element and, therefore, a higher order model for a room space than in the case of earlier approaches, excellent com-

putational efficiency was retained whilst the method overcame the earlier problems associated with the treatment of heat transfer. Essential features of the method are now summarized.

Any construction element can be represented as ‘lumped’ thermal resistances and capacitances and it can be intuitive to visualize the problem as an equivalent electric R – C circuit as shown in Figure 1. This can represent a wall, floor or roof of n layers using two ‘capacitors’, C_i , C_o , and three ‘resistors’, R_i , R_m , R_o .

Using optimization techniques, the share of the two capacitors and three resistors as proportions of their overall values can be arrived at.¹³ The generalized constrained optimization problem can be summarized as follows:

$$\text{minimize}_x: f(x)$$

subject to: $Ax \leq b$ (linear inequality constraints)

$$A_{\text{eq}}x = b_{\text{eq}}$$
 (linear equality constraints)

$$C(x) \leq 0$$
 (nonlinear inequality constraints)

$$C_{\text{eq}}(x) = 0$$
 (nonlinear equality constraints)

$$L_{\text{bound}} \leq x \leq U_{\text{bound}} \quad (1)$$

Where A , A_{eq} , $C(x)$, $C_{\text{eq}}(x)$ are coefficients of the linear and nonlinear equality and inequality constraints and L_{bound} , U_{bound} represent lower and upper limits on the minimized function, x .

The objective function was defined as the sum-square-error between the temperature res-

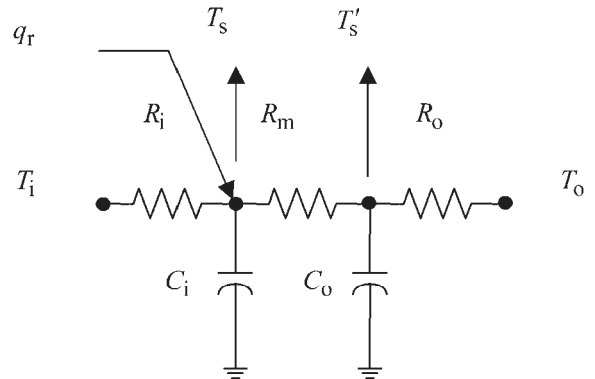


Figure 1 Second-order lumped-parameter construction element

ponse of the second-order construction element (Figure 1) and a high-order 'benchmark' construction element. The order of the high-order benchmark was set at 20 after a comparison between various model orders of up to order 100. Two constraints were set and these were the overall thermal resistance and overall thermal capacitance of the construction element.

Model fitting was carried out for a variety (six) of traditional construction elements ranging from 'high' thermal capacity to 'low' thermal capacity typified by the following:

'High' thermal capacity:	'Low' thermal capacity:
External wall element, brick; insulation; concrete block; plaster	Internal partition element, plasterboard; air space; plasterboard

The spread of results obtained led to the following average resistance and capacitance rationing:

$$R_i = 0.1R_T; R_m = 0.4R_T; R_o = 0.5R_T$$

and

$$C_i = 0.15C_T; C_o = 0.85C_T$$

In which R_T , C_T are the overall resistance and capacitance for the construction element.

Whilst it is not possible to generalize, the results from the six elements were reasonably closely associated with typical variations of 20-30% either side of the mean. Detailed results can be found in Gouda *et al.*¹³ Thus the above results have been used throughout the following, representing the characteristics of a typical construction element.

In Figure 1 note that q_r is a possible radiant source term (e.g., solar radiation). Thus with the notation $\dot{T} = \frac{dT}{dt}$, the circuit can be described by the following energy balances about the internal temperature nodes when substitutions for C_i , C_o and R_i , R_m , R_o are according to the typical model fitting results described above:

$$0.15C_T\dot{T}_s = q_r + (T_i - T_s)/0.1R_T - (T_s - T'_s)/0.4R_T$$

$$0.85C_T\dot{T}'_s = (T_s - T'_s)/0.4R_T - (T'_s - T_o)/0.5R_T$$

Rearranging:

$$\dot{T}_s = \frac{q_r}{0.15C_T} + \frac{T_i}{0.015R_TC_T} - \frac{0.075T_s}{0.06R_TC_T} + \frac{T'_s}{0.06R_TC_T} \quad (2)$$

$$\dot{T}'_s = \frac{T_s}{0.34R_TC_T} - \frac{0.765T'_s}{0.1445R_TC_T} + \frac{T_o}{0.425R_TC_T} \quad (3)$$

Equations (2) and (3) can be expressed in matrix-variable or state space notation:

$$\dot{\mathbf{X}} = \mathbf{A}\mathbf{X} + \mathbf{B}\mathbf{U}$$

$$\mathbf{Y} = \mathbf{C}\mathbf{X} + \mathbf{D}\mathbf{U}$$

In which $\dot{\mathbf{X}}$ is a vector of state derivatives; \mathbf{X} , \mathbf{U} are vectors of state and input variables; \mathbf{Y} is a vector of output variables and \mathbf{A} , \mathbf{B} , \mathbf{C} , \mathbf{D} are matrices of parameters.

Specifically:

$$\begin{bmatrix} \dot{T}_s \\ \dot{T}'_s \end{bmatrix} = \begin{bmatrix} \frac{-0.075}{0.0009R_TC_T} & \frac{1}{0.06R_TC_T} \\ \frac{1}{0.34R_TC_T} & \frac{-0.765}{0.1445R_TC_T} \end{bmatrix} \times \begin{bmatrix} T_s \\ T'_s \end{bmatrix} + \begin{bmatrix} \frac{1}{0.015R_TC_T} & \frac{1}{0.15C_T} & 0 \\ 0 & 0 & \frac{1}{0.425R_TC_T} \end{bmatrix} \times \begin{bmatrix} T_i \\ q_r \\ T_o \end{bmatrix} \quad (4)$$

$$\begin{bmatrix} y_1 \\ y_2 \end{bmatrix} = \begin{bmatrix} 1 & 0 \\ 0 & 1 \end{bmatrix} \times \begin{bmatrix} T_s \\ T'_s \end{bmatrix} \quad (5)$$

$$+ \begin{bmatrix} 0 & 0 & 0 \\ 0 & 0 & 0 \end{bmatrix} \times \begin{bmatrix} T_i \\ q_r \\ T_o \end{bmatrix}$$

A model of a room envelope can now be realized by representing each envelope element by the above with the exception of glazing which was treated as a simple solar transmittance path. This was generated using Simulink in the Matlab environment. A standard state-space block in Simulink was used to implement each element (Figure 2a) and the room space model was completed by adding two first order nodes representing room air temperature and room air moisture content (Figure 2b and c). A solar algorithm (for solar radiation through glazing) was developed as a Matlab function and a one-equation ventilation model were developed as driving inputs together with climate data (external temperature, relative humidity and wind speed) from a meteorological file.

3 Room emitter modelling

Ongoing research into room emitter modelling suggests that a third-order description is an acceptable compromise between model rigour (i.e., relative accuracy) and manageable computational effort (Figure 3).

Convactor-radiators and pure convectors are required to respond to BS EN 442-3 (1997)¹⁴ such that surface-room air emission can be described by an expression which relates heat emission to mean water-to-air temperature difference raised to a power (typically 1.3 for convactor-radiators and 1.5 for pure convectors). A general third-order model for an emitter therefore emerges:

$$C_w \frac{dT_{w1}}{dt} = 3m_w c_p (T_{wi} - T_{w1}) - K(T_{w1} - T_i)^n \quad (6)$$

$$C_w \frac{dT_{w2}}{dt} = 3m_w c_p (T_{w1} - T_{w2}) - K(T_{w2} - T_i)^n \quad (7)$$

$$C_w \frac{dT_{wr}}{dt} = 3m_w c_p (T_{w2} - T_{wr}) - K(T_{wr} - T_i)^n \quad (8)$$

where C_w, K refer to the overall (water and material) thermal capacity and overall emission constant for the emitter. The appearance of overall values for these parameters accounts for the scaling value of 3 in each of the water energy terms in the above. n is the emission index. Each of the above ordinary differential Equations (6–8) can be arranged by selecting a *function* block and an *integrator* block from the Simulink library as was done for the room air node earlier (Figure 4).

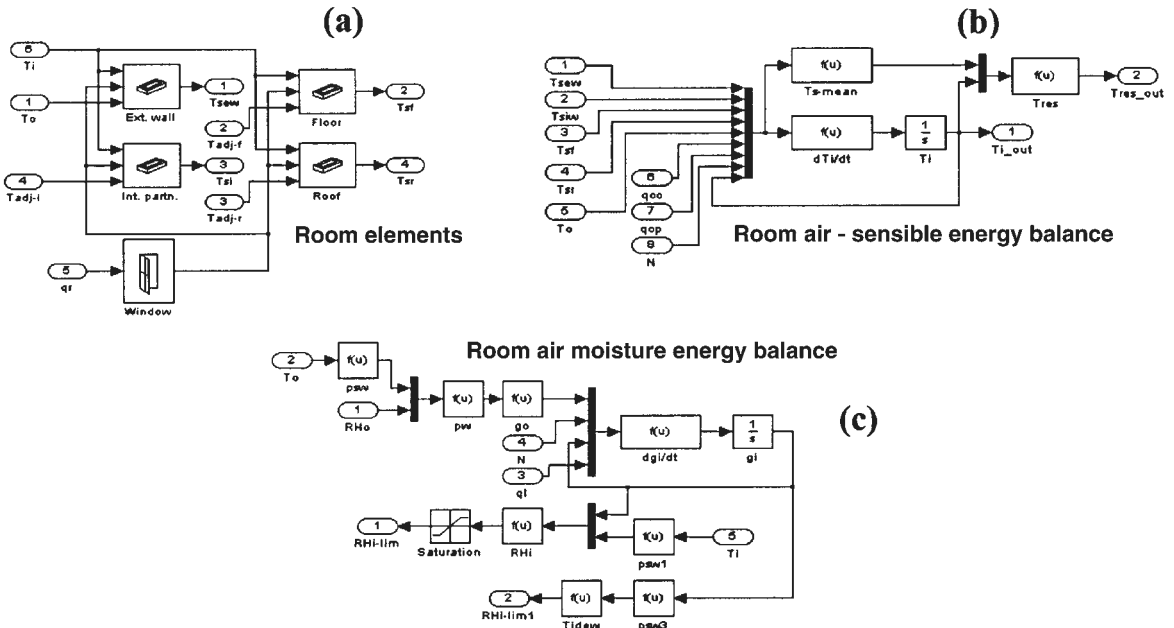


Figure 2 (a) Elements cluster; (b) Temperature node; (c) Moisture content node

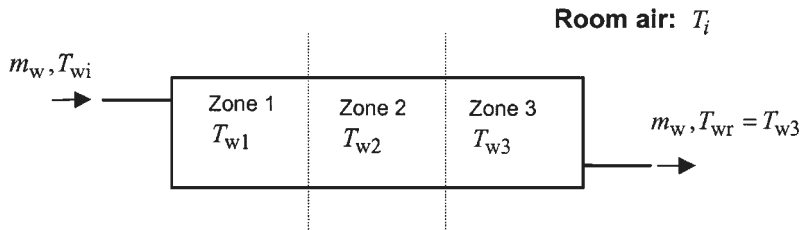


Figure 3 Third-order room emitter

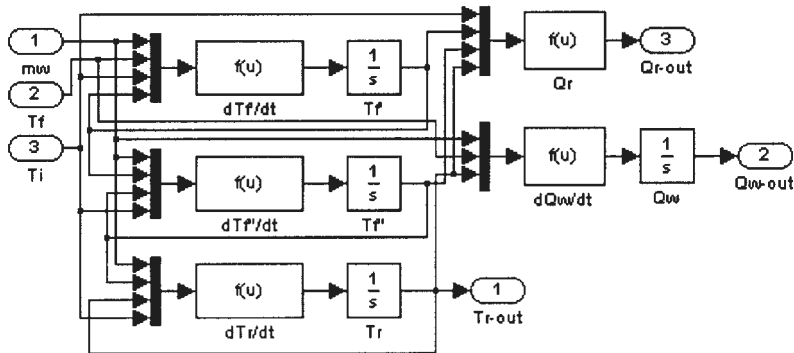


Figure 4 Simulink realization for a room emitter

Of the two additional function blocks (one with an integrator) on the output side, the first of these calculates the overall heat transfer to the room and this therefore forms the required input to the room air energy balance sub-system representing the heating plant source term. The second calculates the heat given up by the water in the heat emitter and, by subsequently integrating this result, the running total energy consumption by the plant.

For chilled ceilings, a similar approach can be used as for hot water emitters. However, the emission characteristic over a wide range of operating conditions tends to be near-linear for many system types due partly to the low water-side temperature differential inherent in such systems. Thus Equations (6–8) are used but with $n = 1$.

4 Modelling the control system

Four further sub-systems are needed in order to complete the treatment of the plant:

- the control valve.

- the valve actuator (i.e., positioning mechanism).
- the measuring instrument (i.e., temperature detector in this case).
- the controller.

4.1 Control valve

For HVAC applications, a logarithmic or *equal percentage* valve characteristic is usually preferred in order to attempt to compensate for the heat emission non-linearity and thus force a more linear control system response overall. For systems with a low water side temperature difference (i.e., such as chilled ceilings) an equal percentage valve may well over-compensate this non-linearity and something close to a linear characteristic might be better.

It is possible to express inherent valve characteristics, G , which describe the normalized flow through the valve as a function of valve position at constant system pressure. From either of these, an installed characteristic, G' , can be derived which expresses the same relationship but at essentially variable system pressure:

$$\text{Equal percentage: } G = f_o^{(1-p)} \quad (9 \text{ a,b})$$

Linear: $G = f_o + p(1 - f_o)$

$$G' = m_{wd}G[G^2(1 - A) + A]^{-\frac{1}{2}} \quad (10)$$

In the above, f_o , p , m_{wd} , and A are the valve let-by (fraction), stem position (fraction), design-rated mass flow rate (kg/s) and valve authority (fraction), respectively.

4.2 Valve positioning devices

Observations in the laboratory suggest that small-to-medium electromechanical valve positioners (i.e., up to about 50 mm valve sizes) track according to a constant rate of change, $\frac{dp}{dt} = \text{Rate}$. The rate of change in valve position is required to be limited to the derivative Rate . Thus for given values of a rising and falling slew rate, R^+ , R^- (per sec), (i.e., $1/R^+$ is the time taken for the valve to move from fully closed to fully open and $1/R^-$ is the time taken for the valve to move from fully open to fully closed) the valve position at time t , $p(t)$, can be calculated from:

$$p(t) = \Delta t R^+ + p(t - 1) \quad (\text{Rate} > R^+) \quad (11)$$

$$p(t) = \Delta t R^- + p(t - 1) \quad (\text{Rate} < R^-) \quad (12)$$

$$p(t) = u(t) \quad (R^- < \text{Rate} < R^+) \quad (13)$$

In Equations (11–13) $u(t)$ is the current value of control signal. Note that the sign of the falling slew rate, R^- , will be negative. The Simulink *rate limiter* block performs this function.

A further consideration is the possibility of mechanical slack leading to hysteresis error in the linkage between the actuator and the valve plug. This occurs when the valve positioning signal reverses direction and a small degree of travel is needed to take up any slack in the linkage before the valve stem starts to move again. This will usually be quite low for small and medium size electromechanically positioned valves but can be quite significant in larger valves and with pneumatic positioners. Use can be made of the *backlash* block in Simulink to model the effect of hysteresis.

Taken together, a Simulink subsystem for the control valve (with the option of equal per-

centage or linear inherent characteristics), positioning device and linkage can be realized as in Figure 5.

4.3 Measuring instruments

Measuring instruments (e.g., temperature detectors, pressure and flow detectors, heat meters, power meters) usually take from a few seconds to a few minutes to register and process the data they measure. For example, sensors mounted in fast-moving liquid streams in pipes will tend to respond quickly (a fraction of one second to a few seconds). On the other hand, a sensor mounted on a room wall measuring air-dry bulb temperature in relatively still air will respond more slowly (a fraction of one minute to a few minutes). It is common for such components to respond exponentially such that a first-order lag characterized by a time constant is generally a good description.

Thus for the room air temperature detector:

$$t_d \frac{dT'_i}{dt} = T_i - T'_i \quad (14)$$

In which T'_i , t_d are the temperature signal from the detector and detector time constant respectively. This can be expressed using the *function* and *integrator* Simulink library components.

4.4 Controller

Model closure arises when the room temperature, T_i , is fed back to a controller and the resulting signal is used to position the control valve and hence govern heating or cooling system output. The general expression for a proportional-integral-derivative (PID) controller is as follows:

$$u = k_p e + k_i \int_0^{\infty} e dt + k_d \frac{de}{dt} \quad (15)$$

Where e , k_p , k_i , and k_d are the error, proportional gain, integral gain and derivative gain for the controller respectively. The three gain values are tunable control parameters (i.e., are adjusted in practice to give 'good' control—usually amounting to a stable response with favorable set-point

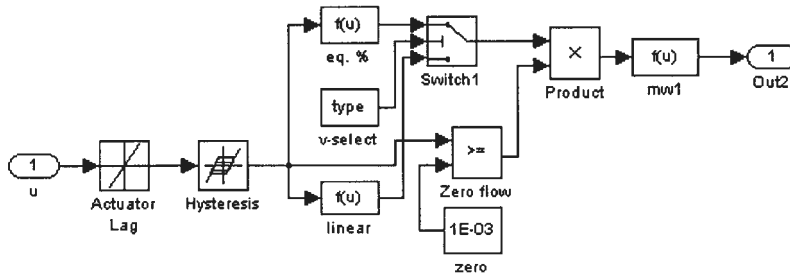


Figure 5 Simulink realization for the control valve

tracking criteria). The control error, $e = T_r - T_i$, where T_r is in this case the reference value or set point in room temperature.

When a PID controller experiences an input error signal which is both large and sustained the integral term gradually accumulates a very large output value. This will occur for example during early morning preheating when the error is large to start with but it also takes some time (sometimes a few hours) for the heating operating at full capacity to bring the control error to within its proportional band. By the end of the preheat period therefore, the integral term will have forced the control signal to a very large value causing actuator saturation. The control variable then overshoots causing the sign of the error to change. This sign change then ensures that the integral signal de-accumulates but it takes time for the signal value to come down sufficiently for the actuator to de-saturate. This ‘stickiness’ problem is called integral wind-up and an anti-wind-up mechanism is needed on most PID controllers likely to experience such periods of operation in order to prevent it from happening. There are a few anti-wind-up strategies but they are all based on the same idea—that of retarding the integral term in some way when the actuator reaches saturation. The simplest thing to do is to saturate the integral term to the upper and lower limits of the control signal that correspond to actuator saturation (i.e., 1 and 0 in this case). This can easily be done in Simulink through the integrator block has a ‘limit output’ facility.

Also a saturation block should be added on the overall control signal output value leaving the con-

troller and limit the signal to 0 (minimum); 1 (maximum). This is because the valve model equations are based on a control signal in the fractional range $0 \rightarrow 1$. Thus any value outside this range is likely to lead to a mass flow rate from the control valve subsystem which is outside the design range hence we adopt a fractional control signal convention accordingly.

Subsystems forming the plant model were grouped together as shown in Figure 6(a) and this grouping was in turn ‘tiled’ into the overall room and plant model as shown in Figure 6(b).

Most of the subsystems have been masked behind dialogue boxes for convenient parameter setting. For example, the mask dialogue box for the heating and chilled ceiling subsystem is shown in Figure 7.

5 Model application

It is possible to obtain optimum PI settings using nominal values as a starting point by minimizing a cost function attached to the target variables T_i . This process is more or less equivalent to using an automated self-tuner on site. In practice, tuning will normally take place in the off-design when the plant is operating around the required set point but at part load conditions simply because it will rarely be convenient to wait for design conditions to prevail before commissioning is carried out. The optimization was therefore carried out using a nonlinear control design (NCD) blockset available from within the Simulink extended program library used at arbitrarily chosen mid-season conditions corresponding to moderate ambient air temperatures.

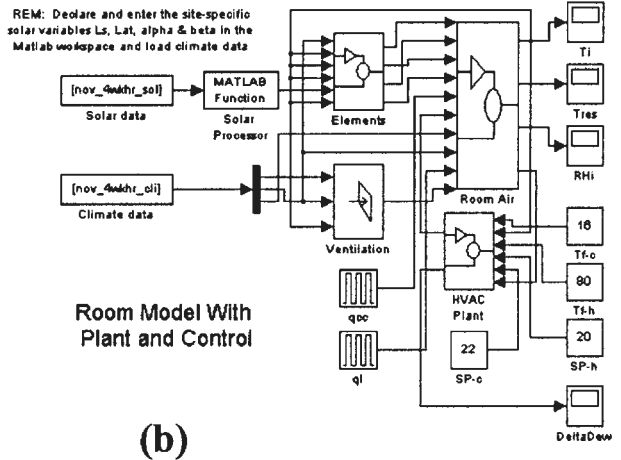
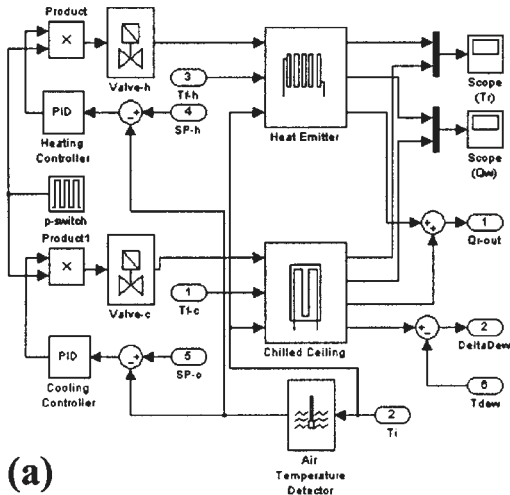


Figure 6 (a) Plant subsystem; (b) Overall room and plant model

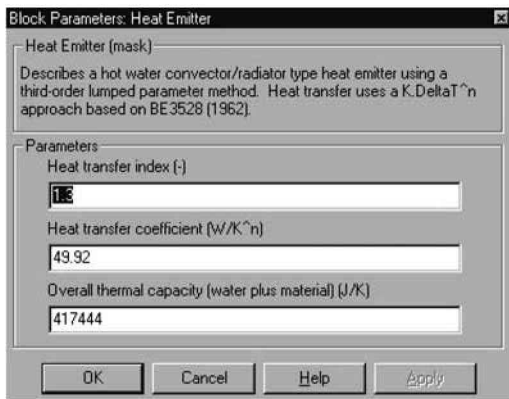


Figure 7 Mask dialogue box for the emitter subsystem

The NCD block works as follows. A constraint envelope is defined that defines upper and lower bounds of the controlled variable, together with one or more tunable variables. A cost function is generated consisting of a weighted maximum constraint violation. At each iteration, each tunable variable is perturbed in turn and the resulting constraint values and cost function are evaluated. A gradient search direction is determined from these results and a line search along the gradient is performed in order to minimize the cost function while simultaneously satisfying the constraint envelope criteria.

Hence the NCD block setup involved the following:

- A constraint envelope was defined for the controlled variable T_i . This consisted of an arbitrary but ‘desirable’ response to a step change in the setpoint from 0 to 20°C.
- The control parameters were set as tunable variables.

The initial parameters of the PID controller used in the heating loop were based on the actual settings applied to the control of heating in a building space on the Northumbria University campus. In addition, the characteristics of this space were, as closely as possible, used as input data for the application of the model. These initial heating controller settings (k_p , k_i , k_d) were 0.1 K, 0.01 K/s, and 0.5 s/K, respectively. Preliminary results suggested that the cooling loop contained substantial damping and was thus found to be unconditionally stable. Therefore, freedom existed to apply a very high value of k_p to achieve offset-free tracking. The preliminary parameters of the PID controller used in the cooling loop (k_p , k_i , k_d) were -100 K, 0 K/s, and 0 s/K, respectively.

As a result of tuning, the locally optimized heating controller parameters were found to be 1.527 K; 0.005 K/s and 0.05 s/K respectively for

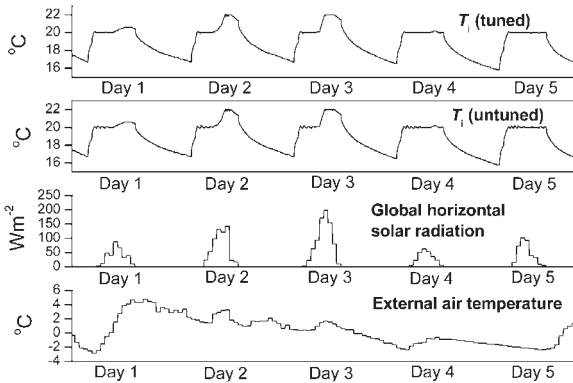


Figure 8 Winter heating response

k_p , k_I and k_d . No improvement to the initial gain for cooling controller was found, confirming its unconditionally stable nature.

A sample of results for the winter heating case is shown in Figure 8. The results show both tuned and untuned PID control (the untuned results based on the initial nominal settings). The untuned responses are actually quite reasonable but tuning has removed the small degree of oscillation evident during tracking. There is clear evidence of a small amount of afternoon overheating on those days in which significant solar radiation are available (global horizontal solar radiation data have been added to confirm this).

A sample of results for the summer cooling case is shown in Figure 9.

Because chilled ceiling systems are designed

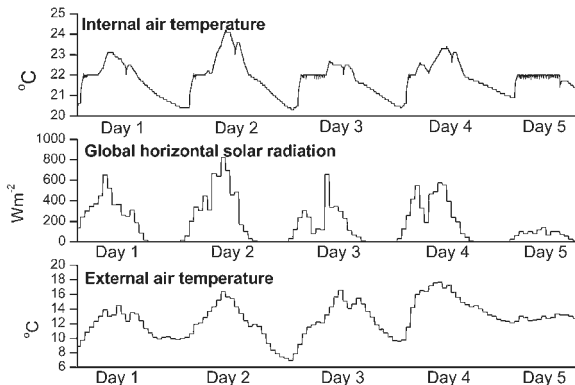


Figure 9 Summer cooling response

to crop peak heat gains in spaces and are not intended to provide close control (not least because of the essential lower limit imposed on surface temperatures to avoid dewing) then, again, there is evidence of afternoon overheating on days with high solar availability. The early morning temperature climb characteristic in the case of summer operation is due to internal casual heat gains.

In order to test the controller's robustness properties, the building construction data were changed to those representing a very low thermal capacity structure while keeping the overall transmittance of each element constant. An assessment of a wide but practical range of material choices suggested that the lowest realistic thermal capacity construction would exhibit element overall thermal capacities of about 20% of the original high thermal capacity case depicted in Figures 8 and 9. Thus the original element thermal capacities were reduced to 20% of their existing values for this test. This would have the effect of making the system more responsive (and, hence control more 'difficult'). This test was carried out for the winter heating case only and controller specifications remained unchanged. Figure 10, reveals that the tuned PID controllers give a reasonable response but with overshoot. Thus a certain amount of robustness of the PID controllers is

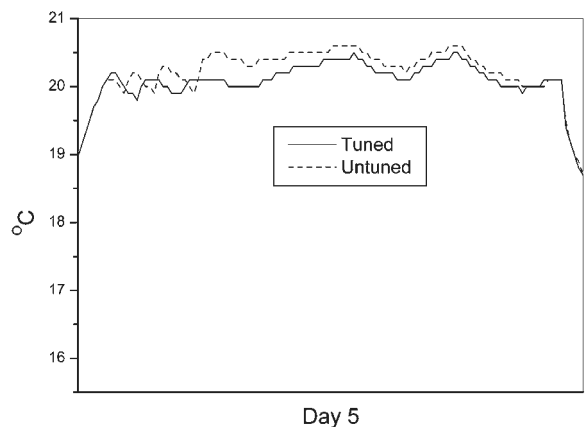


Figure 10 Winter heating response (low thermal capacity construction)

lost, requiring it to be retuned. A greater degree of oscillation is evident in the untuned response and, additionally, tracking is inferior.

The model with a single building zone was found to have good computational efficiency—typically 3 h of simulation time per second of processor time on a Pentium 350Mhz PC using a stiff variable step solver, though the processor times were considerably higher than this with fixed step solvers.

6 Conclusions

A simulation model of the thermal performance of a building with HVAC plant and control has been developed as a test bed for analyzing control strategies.

A new approach to building space modelling is described and implemented, based on parameter-optimized second-order descriptions of each building envelope element. Subsystem models of secondary HVAC plant and control were also developed making use of an existing component library where possible. The result is a detailed dynamic model of a building space with HVAC plant and control which enjoys flexibility, transparency and computational efficiency essential for the specialist case of investigating control system response over low time scales. Model application has been demonstrated involving detailed simulations of controller tuning and response.

Further work is warranted on extending the component library to include other HVAC component classes, together with the need to do some work on model validation.

References

- 1 *TRNSYS: A transient system simulation program*, Volume 1 (reference manual). Solar Energy Laboratory, University of Wisconsin, Madison, WI, 1996.
- 2 Clark DR. *HVACSIM+ Building System and Equipment Simulation Program Reference Manual: NBSIR 84-2996*. Gaithersburg, MA: National Institute of Standard Technology, 1985.
- 3 *SIMBAD: Building and HVAC Toolbox*. Centre Scientifique et Technique du Batiment, 1999.
- 4 Underwood CP. *Documentation of TRNSYS Component Models for HVAC Applications*. Built Environment Research Group, University of Northumbria, Newcastle upon Tyne, 1994.
- 5 Dexter AL, Eftekhari MM, Haves P, Jota FG. The use of dynamic simulation models to evaluate algorithms for building energy control: experience with HVACSIM+. Proceedings of ICBEM'87: International Congress on Building Energy Management, Lausanne, 1987.
- 6 Metcalf RM, Taylor RD, Pedersen CO, Liesen RJ, Fisher DE. Incorporating a modular simulation program into a large energy analysis program: The linking of IBLAST and HVASIM+. Proceedings of Building Simulation '95, Madison, WI, 1995.
- 7 Adams S, Holmes MJ. Determining time constants for heating and cooling coils: BSRIA Technical note TN6/77. Building Services Research and Information Association, Bracknell, 1977.
- 8 Shavit G, Brandt SG. The dynamic performance of discharge air temperature system with PI controller. *ASHRAE Trans.* 1982; 88: 826-38.
- 9 Brath P, Rasmussen H, Haggalund T. Control of the outlet air temperature in an air handling unit. Proceedings of the UKACC International Conference: Control'98, London, 1998.
- 10 Underwood DM, Crawford RR. Dynamic nonlinear modelling of a hot water to air heat exchanger for control applications. *ASHRAE Trans.* 1991; 97: 49-55.
- 11 Lorenz F, Masy G. Methode d'évaluation de l'économie d'énergie apportée par l'intermittence de chauffage dans les batiments. Traitement par differences finies d'un model a deux constantes de temps: Report no. GM820130-01. University de Liege, Belgium, 1982.
- 12 Tindale A. Third-order lumped-parameter simulation method. *Building Serv. Eng. Res. Technol.* 1993; 14: 127-37.
- 13 Gouda MM, Danaher S, Underwood CP. Building thermal model reduction using nonlinear constrained optimization. *Build. Environ.* 2002; 37: 1255-65.
- 14 BS EN 442-3: Specification for radiators and convectors—evaluation of conformity. British Standards Institute, London, 1997.